

Full length article

Subsurface profiling along Banni Plains and bounding faults, Kachchh, Western India using microtremors method



Dhananjay A. Sant^{a,*}, Imtiyaz A. Parvez^b, Govindan Rangarajan^c, Satish J. Patel^a,
Madhuri N. Bhatt^a, T.A. Sanoop Salam^a

^a Department of Geology, Faculty of Science, The Maharaja Sayajirao University of Baroda, Vadodara 390002, India

^b CSIR Fourth Paradigm Institute (Formerly CSIR Centre for Mathematical Modeling and Computer Simulation (C-MMACS)), NAL Belur Campus, Bengaluru 560 037, India

^c Department of Mathematics, Indian Institute of Science, Bangalore 560 012, India

ARTICLE INFO

Keywords:

Banni Plains, Kachchh Mainland Fault

Microtremor

Ambient noise

Fundamental resonant frequency

H/V spectral ratio

Positive flower structure

ABSTRACT

The present article is a maiden attempt to map shallow subsurface rheological interfaces laterally across the Banni Plains and to decode geometry of the antecedent faults associated with the Kachchh Mainland Fault using the microtremor method. We conducted microtremor data acquisition for thirty-one sites along N-S transect from Loriya in Mainland Kachchh to Bhirandiara towards Patcham Island. Results from H/V spectral ratio technique show presence of two distinct rheological interfaces characterised by the resonant frequency (f_r) ranges 0.23–0.27 Hz and 0.8252–1.5931 Hz respectively. The above frequency ranges are correlated with the depths of the Mesozoic-Basement (M-B) interface and the Quaternary-Tertiary (Q-T) interface. Using either the velocity (V_s) of seismic waves at the M-B and Q-T interfaces (calculated as 1830 m/s and 411 m/s respectively) or the standard non-linear regression relationship derived for the Banni Plains ($h = 110.18f_r^{-1.97}$) we estimate the depth range for M-B interface to be 1442–1965 m and for Q-T interface to be 44–160 m. The subsurface profile across the Banni Plains educe cluster of four faults that develop an array of imbricate faults at the forefront of the Kachchh Mainland Fault within the Banni Footwall Syncline. The geometry of the faults suggests a 'positive flower structure' indicating step-overs and strain restraining bends displaying push-ups resulting from localized shortening between converging bends of Kachchh Mainland Fault and the South Wagad Fault. The Banni Footwall Syncline preserves evidence of two episodes of deformations. The initial deformation event led to subsidence within the Kachchh Mainland Fault Zone bringing Mesozoic sequence juxtaposed to the basement rocks, whereas the later event is dominated by an uplift developing a positive flower structure in the Kachchh Mainland Fault Zone. Finally, the present study provides a mechanism to investigate faults and fault geometries correlating surface structural grains with subsurface structures.

1. Introduction

The Rann of Kachchh forms a vast E-W trending depression developed between the Nagarparkar Fault (NPF) in the north and an arcuate Kachchh Mainland Fault (KMF) in the south along the Indo-Pak border, Western India (Fig. 1A; Biswas and Deshpande, 1970; Biswas, 1987, 2005). A structural inversion had begun in the Rann of Kachchh during the Tertiary period and has continued to till date (Mathew et al., 2006; Karanth and Gadhavi, 2007). The active growth of several E–W trending faults controls the basin architecture and strain augmentation (Malik et al., 2008). With reference to the 'Median High' (a N–S to NNE–SSW trending subsurface feature across the Kachchh Basin: Biswas, 1982, 1987), the western Rann of Kachchh is substantially wide

compared to the eastern counterpart. The eastern Rann of Kachchh exposes several fault-bounded islands viz., Patcham, Khadir, Bela and Chorar along its axial-part followed by a narrow complex basin. In reference to KMF, Karanth and Gadhavi (2007) referred to the Banni Plains as 'Banni Footwall Syncline' or 'Banni Half Graben'. The Banni Footwall Syncline, the Wagad Block and the Samathiyali Basin are the few interesting segments within the eastern Rann of Kachchh. The epicentre of the Bhuj earthquake (26th January 2001; 23.41°N, 70.23°E; Mw = 7.7; 2001) was located in the eastern segment of the Rann of Kachchh between KMF and the South Wagad Fault (SWF).

Several geophysical studies have been pursued to decode the structure and stress field in the Kachchh Basin viz., electrical imaging (Sastri et al., 2008); electromagnetic radiation investigations (Mathew

* Corresponding author.

E-mail address: sant.dhananjay-geology@msubaroda.ac.in (D.A. Sant).

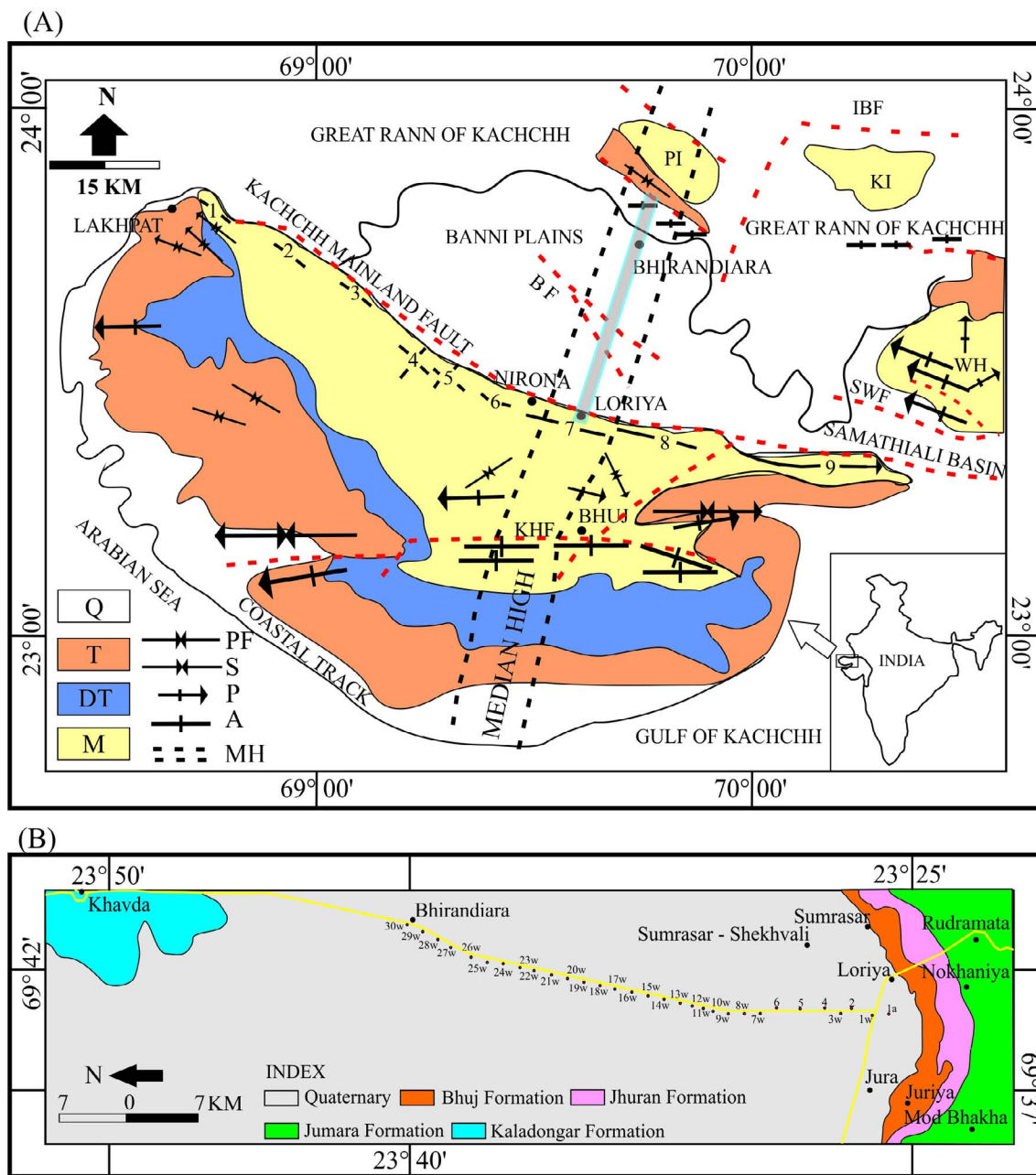


Fig. 1. (A) Geological and geomorphological map of Kachchh Peninsula showing important stratigraphic units, structural elements, landforms, and key locations referred in text (Biswas, 2005). Codes used in Map: Q – Quaternary sediments, T – Tertiary sediments, DT – Deccan Traps, M – Mesozoic sediments; PF – Plunging Fold, S – Syncline, P – Plunge, A – Anticline, MH – Median High; 1. Guneri Dome, 2. Mudhan Dome, 3. Jara Dome, 4. Jumara Dome, 5. Nara Dome, 6. Keera Dome, 7. Jhura Dome, 8. Habbo Dome and 9. Khirsar Dome. Star represents epicentre of 2001 Bhuj earthquake. PI – Pachcham Island, KI – Khadir Island, WH – Wagad Highland; IBF – Island Bet Fault, BF – Banni Fault, SWF – South Wagad Fault, KHF – Katrol Hill Fault. (B) Geological map of Banni Plain between Mainland Kachchh and Patcham Island showing location of stations for microtremor measurements (1–31) along Loriya to Bhirandiar transect. The stations are spaced at 30-second interval (~1 km).

et al., 2006; Mallik et al., 2009); magnetotelluric studies (Naganjaneyulu et al., 2010; Chandrasekhara et al., 2012); heat flow studies (Vedanti et al., 2011); seismological studies (Chung and Gao, 1995; Mandal, 2007; Mandal and Hurton, 2007; Antolik and Dreger, 2003); measurement of H/V resonant frequency (Mandal et al., 2005; Chopra and Choudhury, 2011; Kumar et al., 2012; Chopra et al., 2013 and Singh et al., 2014). However, mapping of subsurface extension of faults and analogous structures up to shallow depths developed because of neotectonic activity using geophysical techniques is also essential (Karanth and Gadhavi, 2007).

In this study, we have investigated subsurface stratified as well as fault-controlled sediment/rock interfaces in the Banni Plains using the microtremor (ambient noise) as the Surface waves are generated by

persistent ambient noise within the region. The Surface waves generated have strong acoustic impedance along the sediment/rock interface having contrasting density and therefore exhibit a prominent resonating frequency corresponding to this interface (Kanai, 1957; Yamanaka et al., 1994; Ibs-von Seht and Wohlenberg, 1999; Delgado et al., 2000; Parolai et al., 2002; Garcia-Jerez et al., 2006; Zhao et al., 2007; Rošer and Gosar, 2010). The growing popularity of the microtremor method is due to its cost effectiveness and a rapid tool for approximation of depths for the subsurface interfaces. Microtremor studies provide an opportunity to infer results as a 2-D cross section when carried out along a profile and as 3-D when carried out under a grid pattern (Sukumaran et al., 2011). The resolution of the study varies with the topography of the terrain and purpose. In summary, subsurface

mapping of rock/sediment interface, faults and plutons are feasible using microtremor method (Zhao et al., 2007; Dinesh et al., 2010; Sukumaran et al., 2011; Paudyal et al., 2013; Joshi et al., 2017).

We compared the fundamental resonant frequencies with the prominent interfaces in the Deep Banni Core A (DGH Records). The result of microtremor studies enabled us to (i) determine the Quaternary-Tertiary and the Mesozoic-Basement interfaces (ii) estimate thickness of the Quaternary sediment and the Tertiary-Mesozoic sedimentary (iii) report the absence of the Deccan basalts underneath the Banni Plains and (iv) delineate geometry of the antecedent faults in the Banni Footwall Syncline and their characteristics. Such an interdisciplinary, cost-effective and quick study that reveals the third dimension of faults/fault geometry within the fault zones up to shallow depths widens the scope of studies pertaining to recent deformation/active boundaries and their societal effect.

2. Geology and structure

The Kachchh Basin between latitude 22°30'N and 24°30'N and longitudes 68°E and 72°E preserve diverse rocks including sedimentary sequences belonging to Mesozoic and Cenozoic era. The Mesozoic sedimentary lie unconformable on the Precambrian basement (Bardan and Datta, 1987; Biswas, 1987). The only exposed Precambrian rocks reported are from Nagarparkar region (Pakistan) northeast of the study area (Kazmi and Khan, 1973; Khan et al., 2012) and at Meruda, north of Khadir island (Biswas and Deshpande, 1968). Late Cretaceous-early Paleocene mafic plutons and dykes emplace the Mesozoic sedimentary belonging to both early and late Deccan Trap phases. Emplacement of mafic magma during early phase of Deccan Traps resulted in domal structures along the northern periphery of the Kachchh Mainland Hill Range (around Guneri, Mundhan, Jara, Jumara, Nara, Keera, Jhura, Habo and Khirsar: Fig. 1A) resulting in an uplift and restricting the flows of Deccan basalt further south and along the intra-domal depressions. The western periphery of the Kachchh Peninsula, periphery of island belts (Patcham, Khadir, Bela and Chorar Islands) and Wagad Highland expose Tertiary sequence whereas its subsurface extension is traced under the Rann of Kachchh (Figs. 1A, B and 2A and Table 1).

The Kachchh Peninsula is bounded by Nagarparkar Fault (NPF); Island Belt Fault (IBF); Allah Bund Fault (ABF); South Wagad Fault (SWF); Kachchh Mainland Fault (KMF) and Katrol Hill Fault (KHF) (from north to south in Fig. 1A; Biswas and Deshpande, 1970; Biswas, 1987, 2005). NPF restricts the Precambrian to its north and defines the northern extreme of the Rann of Kachchh depression; KMF marks the southern limit of the Rann of Kachchh; IBF defines the northern periphery of the Island belt; ABF is a possible western extension of IBF or segment of NPF whereas the Banni Fault lies in between the Patcham island and the Mainland Kachchh. Further east, cluster of faults characterises the Wagad Block where SWF is the most prominent fault bounding southern fringe of the Wagad Block. The Kachchh Mainland and the Wagad Blocks have dextral strike-slip relationship (Biswas and Khatri, 2002). Both these faults (KMF and SWF) have distinct E–W trending and topographic expression (Mathew et al., 2006). The fading KMF is likely to converge with SWF where KMF step to north, and SWF forms a step-over continuation of the KMF (see Fig. 7 in Biswas and Khatri, 2002 and Fig. 6 in Biswas, 2002). In the Mainland Kachchh, KHF marks the northern periphery of the Katrol Hill.

Geomorphologically, the Banni Plains aggraded between KMF and IBF. It is roughly flat, saline grassland covering an area about 3000 sq. km with a gentle north-westerly gradient. The southern fringes (along KMF) show development of alluvial fans along the mouth of northerly flowing streams emerging across the Kachchh Mainland (Kar, 1993; Chowksey et al., 2011). Two distinct landforms viz., raised mudflats (region ≤ 5 m) and pediments (region ≥ 12 m) characterise the Banni Plains. In general the Banni Plains comprises of fluvio-marine sediments (Kar, 2011) (Fig. 1A and B).

Two deep cores namely, the Deep Banni Core A (1764 m deep from

the surface, along the northern fringe of the Banni Plain, southeast of Birandiyara) and the Deep Nirona Core B (2224 m deep from the surface, along the southern fringe of the Banni Plain, West of Loriya village) describe the subsurface geology of the Banni Plains. The Deep Banni Core A reveals the presence of a granite basement at a depth of 1688 m (Fig. 2A) whereas the Deep Nirona Core B encounters the trachytic basement at depth of 2200 m. The estimated thickness of stratigraphic sequences from two DGH records suggests the Banni Basin comprises Mesozoic sedimentary (Banni Core A: 1310 m; Nirona Core B: 1278 m), Neogene sedimentary (Banni Core A: 504 m; Nirona Core B: 413 m) and Quaternary sediments (Banni Core A: 100 m; Nirona Core B: 506 m).

Biswas (1999) discussed subsurface extension of the Jumara Formation (Callovian-Oxfordian) further north of the Mainland Kachchh as well as extension of the Kaladonger Formation (Aalenian to Bathonian) further south from the Patcham Island into the Banni Plains. The Banni fault in the region is inferred based on juxtaposition of younger Jumara Formation with the older Kaladonger Formation where, the southern side of the Banni Fault has gone done by about 300 m (Fig. 1). Further, the Miocene sediments have uniformly aggraded across the basin. Two shallow cores viz., north of Dhordo (60 m depth) and northeast of Berada (51 m depth) in the Banni Plains elucidate the late Quaternary sequence. These sediment sequences show intercalation of clayey-silt and silty-clay (Maurya et al., 2013). The litho-stratigraphic records procured from the deep and shallow cores suggest that the Banni Basin got initiated during early Miocene that continued in Quaternary.

3. Microtremor studies

Several studies have shown that the ambient noise encapsulates fundamental resonant frequency of the sediment layers (Ohta et al., 1978; Celebi et al., 1987; Lermo et al., 1988; Field et al., 1990; Hough et al., 1991; Konno and Ohmachi, 1998; Aki and Richards, 2002). These resonant frequencies derived from the microtremors show strong correlation with the velocity of the Rayleigh waves and the thickness of the sediments (Ibs-von Seht and Wohlenberg, 1999; Parolai et al., 2002). To characterise amplification of the seismic wave for a given site, Nogoshi and Igarashi (1971) proposed a technique to normalize the source effect by taking the spectral ratio of the horizontal (NS + EW component) to the vertical component (H/V) of the noise spectrum. Nakamura (1989) further popularized the method and its applications. Field and Jacob (1993), Parolai and Galiana-Merino (2006), Bonnefoy-Claudet et al. (2006), Garcia-Jerez et al. (2006), Zhao et al. (2007), Nakamura (2008), Bard (2008), Pilz et al. (2009), Lunedei and Albarello (2010), Sánchez-Sesma et al. (2011) carried out extensive studies to assess integrity of this method with several modifications.

We carried out microtremor measurements for thirty-one sites spaced at 30-second intervals (~ 1 km) along the N-S to NNE-SSW transect starting from the village Loriya (Mainland Kachchh) to the village Bhirandiyara (towards Patcham Island) across the Banni Plain (Fig. 1B). The profile coincides with the Median High. We deployed a Lennartz seismometer (5 s period) and a City Shark-II data acquisition system to acquire ambient noise of three components viz., NS, EW, and vertical directions. The duration of recording continued for 40 min at the rate of 100 samples/sec (see Fig. 3 in Sukumaran et al., 2011). GEOPSY software (SESAME European Project, 2004) was used to compute the ratio between the Fourier amplitude spectra of the H/V components of persisting Rayleigh waves from the ambient noise acquired from all thirty-one sites (Fig. 1B).

The H/V spectral ratios were plotted between 0.2 Hz and 30 Hz including the complete range of resonating frequencies recorded within the study area (Fig. 3). Customised Matlab code determined statistically significant spectral peaks (one standard deviation greater than the baseline activity) for H/V spectral ratios. These peaks then corresponded to significant frequencies for each station. The significant frequencies f_0 , and f_1 were singled out for the individual stations based

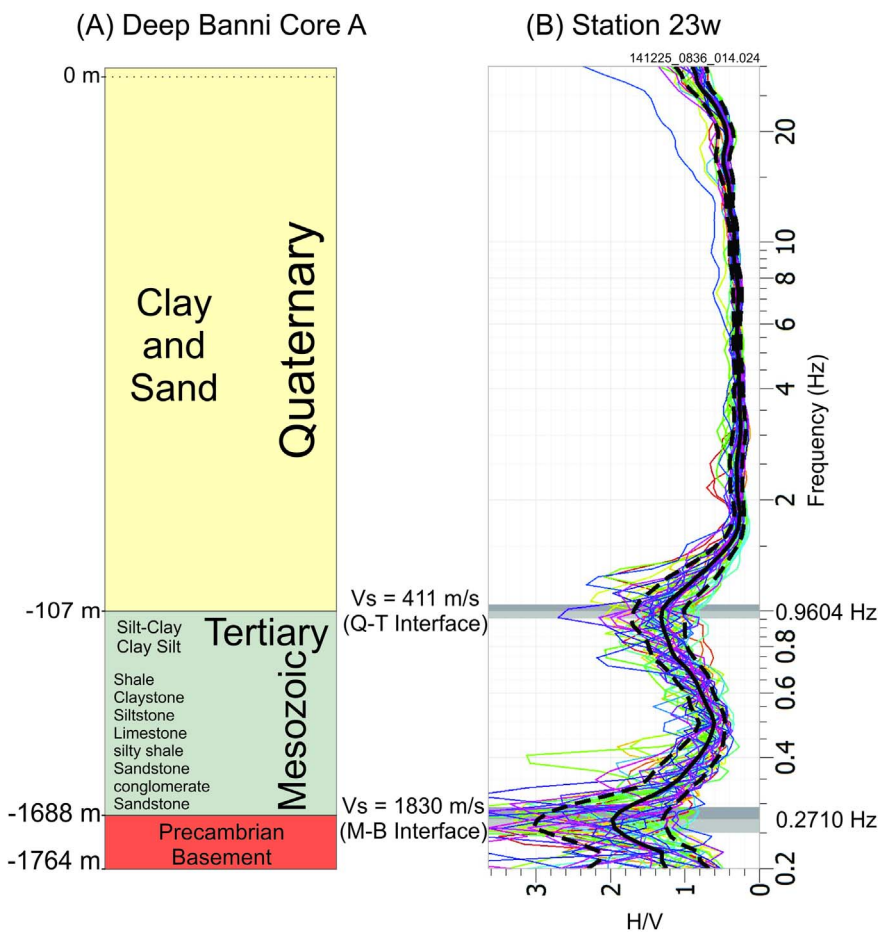


Fig. 2. Comparison of fundamental resonant frequency 0.9604 Hz and 0.271 Hz characterising station 23w with Q-T and M-B interface along Deep Banni Core A. The values of frequency and depth substituted in Eq. (2) provide theoretical velocity V_s at Q-T and M-B interfaces (Table 2).

on amplitudes (Fig. 3, Table 2). Fig. 3 illustrates representative H/V spectral frequency plots recorded from the study area.

Theoretical estimation of the thickness (h) of the soil or the sediment layer over the bedrock was linked to the fundamental resonant frequency (f_r) of H/V spectral ratio by an allometric function as given by Ibs-von Seht and Wohlenberg (1999).

$$h = af_r^b \tag{1}$$

where a and b are obtained by performing a nonlinear regression between the thickness and the fundamental resonant frequency.

For a given fundamental resonant frequency, if the velocity of seismic waves (V_s) for a given interface is known, the depth of the interfaces is given by (Parolai et al., 2002)

$$h = \frac{V_s}{4fr} \tag{2}$$

On the other hand, if the depth of the interface in known based on available core records, the velocity of seismic waves (V_s) can be determined using Eq. (2).

The most prominent frequencies procured from the microtremor measurements fall in range from 0.8252 Hz to 1.5931 Hz (recorded along all thirty-one stations). Of the thirty-one stations, 18 stations recorded a single peak at a fundamental frequency between 0.8252 Hz and 1.5931 Hz (f_0). Thirteen stations showed two prominent peaks where one of peaks falls in the frequency range (f_0 , or f_1) between 0.8252 Hz and 1.5931 Hz. The other peak occurs at a frequency that varies with station: 0.23 Hz and 0.29 Hz (8 stations), less prominent frequency 3.9618 Hz (station, 1w) and within range of 27.1119 Hz and 25.7738 Hz (4 stations). In general, the results show the presence of two prominent ranges of frequencies suggesting a three-layer model for the Banni Plains (Figs. 2 and 3 and Table 2).

Station 23w (23°37'N and 69°41'12"E) occurs close to Deep Banni Core A (DGH record). Since the depths of the various interfaces are known for the Deep Banni Core, we used them to correlate the frequencies decoded for this station with appropriate interfaces as follows: (i) 0.271 Hz (f_0) with the interface between Mesozoic sedimentary (Jurassic sequence) and Basement (Precambrian Granite) at a depth of 1688.4 m (referred to as M-B interface) and, (ii) 0.9604 Hz (f_1) with the interface between unconsolidated Quaternary sediment and consolidated Tertiary sedimentary sequence at a depth of 107.1 m (referred to as Q-T interface) (Fig. 2).

The theoretical values of V_s (1830 m/sec and 411 m/sec) were calculated for M-B and Q-T interfaces by substituting their depths along with their corresponding resonant frequencies in Eq. (2) (Table 2). Assuming that these theoretical values for V_s at the M-B and Q-T interfaces are approximately the same for all other stations, we next calculated the depths of these two interfaces for these stations by substituting V_s and resonant frequency in Eq. (2). We also arrived at the following alternative general equation to determine depths for any rheological interfaces, in the Banni Plains using a scatter plot of frequency versus theoretical depth (Fig. 4, Table 2).

$$h = 110.18f_r^{-1.97} \tag{3}$$

Thus, we obtained two different methods for calculating the depths of M-B and Q-T interfaces for different stations. These are compared in Table 2 and Fig. 5.

The signature of the M-B interface is most prominent along eight stations located along the northern extremes of the profile (Fig. 1B; Table 2). The interface marks the contact of Mesozoic sedimentary with that of Basement rocks at depths between 1442 m and 1965 m. The M-B interface is rugged and seems to be below the sensitivity limits of the instruments used in the present survey between stations 1a to 19w

Table 1
Lithostratigraphy of Kachchh Basin (after Biswas, 1992, 2016).

AGE	Kachchh Mainland Group	Patcham Island Group	Eastern Kachchh Group		
			Khadir-Bela-Chorar Islands	Wagad Highland	
Quaternary deposits					
Miocene	Pliocene	Neogene deposits			
	Langhian to Messinian				SANDHAN
	Burdigalian				-- <i>Disconformity</i> -- CHHASRA
Oligocene	Aquitanian				KHARI NADI
	Chatian				-- <i>Unconformity</i> -- MANYARA FORT
Eocene	Rupelian				
	Priabonian				- <i>Paraconformity</i> - FULRA LIMESTONE
	Bartonian				
	Lutetian				HARUDI - <i>Paraconformity</i> -
Paleocene	Ypresian				NAREDI
	Thanetian	-- <i>Disconformity</i> -- MATANOMADH			
Cretaceous	Danian	-- <i>Disconformity</i> -- DECCAN TRAPS			
	Maastrichtian				
	Albian				
	Aptian	BHUJ			
	Hauterivian to Berriasian				
Jurassic	Tithonian	JHURAN			
	Kimmeridgian	<i>Hiatus</i>			
	Oxfordian	JUMARA			
	Callovian	MODAR HILL			
	Aalenian to Bathonian	JHURIO			
		GORADONGAR	GADHADA	WAGAD SANDSTONE	
		KALADONGAR	KHADIR	WASHTAWA	
				Not exposed	
Basement not exposed					

(Figs. 1B and 5). The general thickness of the Tertiary-Mesozoic sedimentary sequence inferred along the transect range from 1624 m to 1841 m (Figs. 5 and 6 and Table 2).

The Q-T interface is a well-established signature along all thirty-one stations. The Q-T interface correlates with interface where unconsolidated Quaternary sequence of clay-sand overlies semi consolidated silt and clay units belonging to late Neogene period at depth

ranging from 44 m to 160 m. The Q-T interface shows moderate to rolling profile except within the Kachchh Mainland Fault Zone (KMFZ). Generally, the thickness of the Quaternary sediment inferred along present transect is from 35 m to 155 m (Figs. 5 and 6).

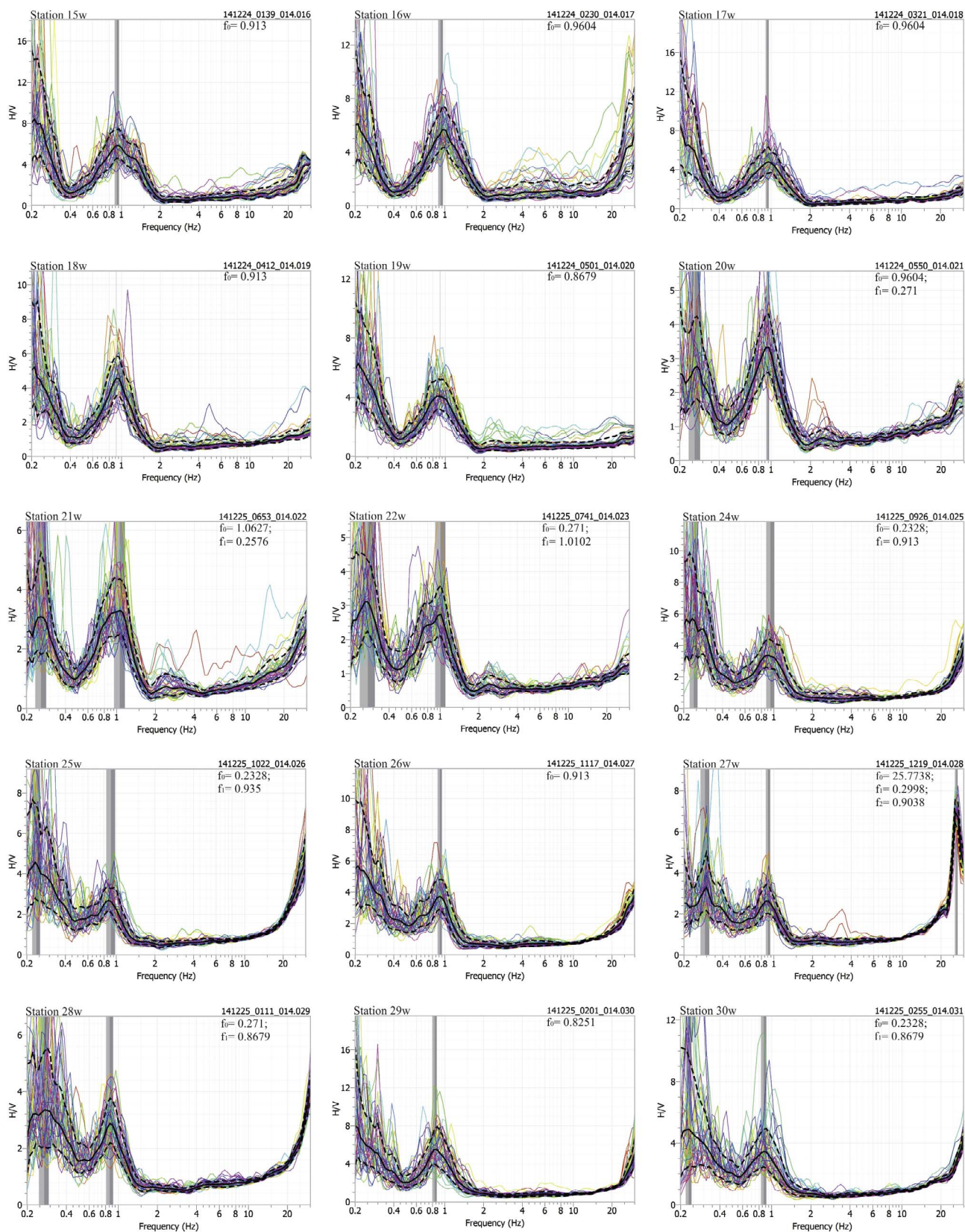


Fig. 3. Scatter plot of H/V versus fundamental resonant frequency for all stations. The figure on right hand top shows frequency peaks (f_0 and f_1) at one-sigma significance.

4. Discussion

The frequency record generated through microtremor studies for thirty-one stations along Loriya –Bhirandiara profile successfully

distinguishes lateral extension of both Q-T interface as well as M-B interface in subsurface (Figs. 5 and 6). The study provides evidence for the absence of Deccan basalt flows in the subsurface of the Banni Plains where the Neogene sequence directly overlies unconformably on the

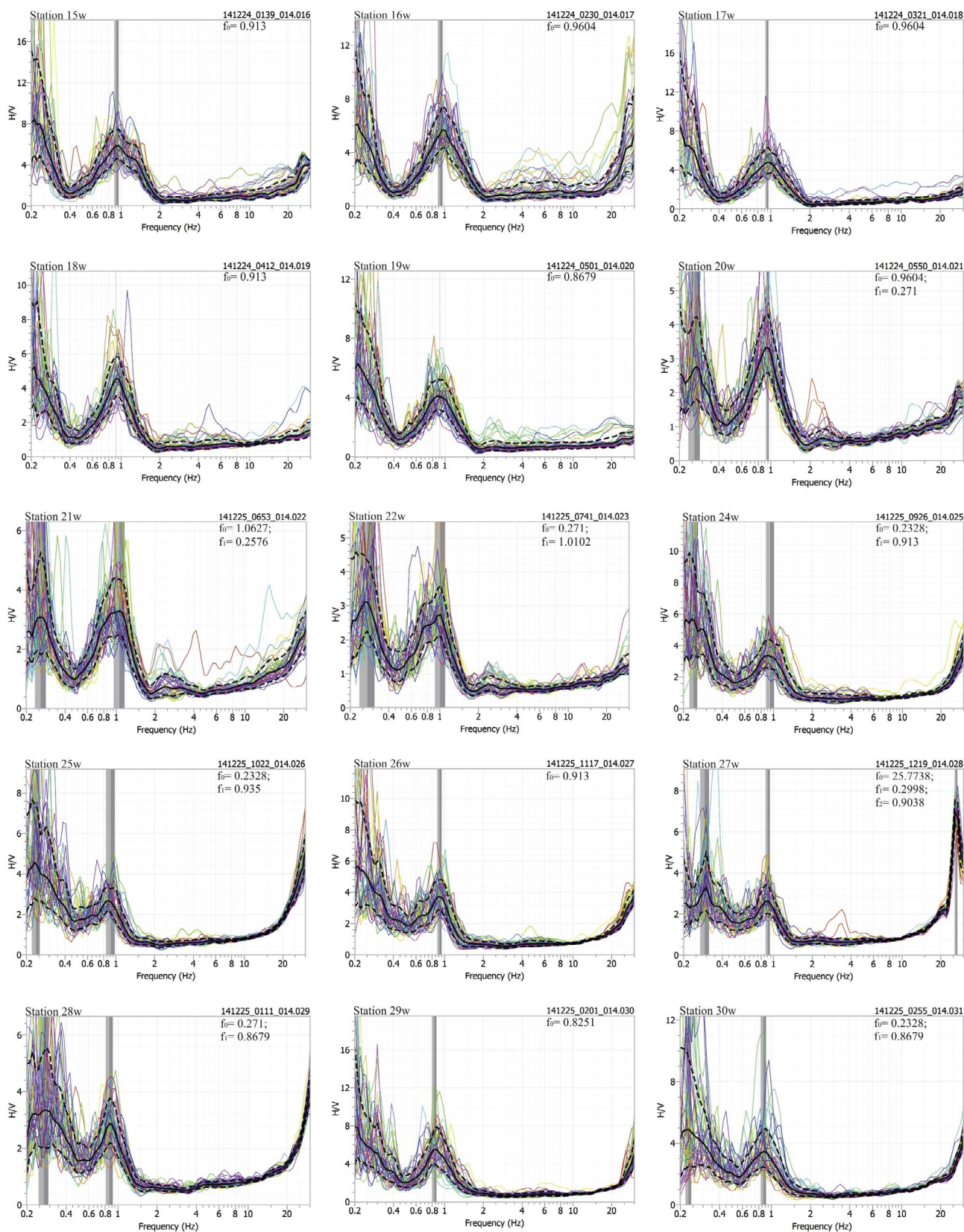


Fig. 3. (continued)

Mesozoic sequence. The emplacement of late Cretaceous mafic plutons at various locations viz., Guneri, Mudhan, Jara, Jumara, Nara, Keera, Jhura, Habbo, and Khirsar (Fig. 1A), have deformed exposed Mesozoic sedimentary in the form of single/multiple domal structures along the

Kachchh Mainland Hill Range (Sen et al., 2016). The geological relationship of these domes with KMF clearly suggests the presence of pre-intrusive arcuate structure through which the magma got emplaced. The latter event further reinstated KMF along pre-existing

Table 2

The table displays fundamental resonant frequency f_0 and f_1 for thirty-one stations across Loriya to Bhirandiara Profile, Banni Plains; The depths for M-B and Q-T interfaces are calculated are based on (1) theoretical values of V_s (1830 m/sec at the M-B interface and 411 m/sec at the Q-T interface) and (2) a general equation for the Banni Plains ($h = 110.18f_1^{-1.97}$).

Station	Frequency (Shallow)	Depth Based On ($V_s=411$ m/sec) (in Meters)	Depth Based On ($110.18f_1^{-1.97}$) (in Meters)	Frequency (Q-T Interface)	Depth Based On ($V_s=411$ m/sec) (in Meters)	Depth Based On ($110.18f_1^{-1.97}$) (in Meters)	Frequency (M-B Interface)	Depth Based On ($V_s=1830$ m/sec) (in Meters)	Depth Based On ($110.18f_1^{-1.97}$) (in Meters)
1a	27.11	3.79	0.17	1.24	83.07	72.48			
1w	3.96	25.94	7.32	1.18	87.38	80.07			
2				1.30	78.97	65.60			
3w				1.24	83.07	72.48			
4				1.24	83.07	72.48			
5	27.11	3.79	0.17	0.96	106.99	119.31			
6				0.87	118.39	145.65			
7w				1.59	64.50	44.02			
8w				1.59	64.50	44.02			
9w				1.51	67.84	48.64			
10w				1.24	83.07	72.48			
11w				1.24	83.07	72.48			
12w				1.18	87.38	80.07			
13w				0.96	106.99	119.31			
14w	25.77	3.99	0.18	0.91	112.54	131.82			
15w				0.91	112.54	131.82			
16w				0.96	106.99	119.31			
17w				0.96	106.99	119.31			
18w				0.91	112.54	131.82			
19w				0.87	118.39	145.65			
20w				0.96	106.99	119.31	0.27	1688.19	1442.62
21w				1.06	96.69	97.74	0.26	1776.01	1594.19
22w				1.01	101.71	108.00	0.27	1688.19	1442.62
23w				0.96	106.99	119.31	0.27	1688.19	1442.62
24w				0.91	112.54	131.82	0.23	1965.21	1946.02
25w				0.94	109.89	125.78	0.23	1965.21	1946.02
26w				0.91	112.54	131.82			
27w	25.77	3.99	0.18	0.90	113.69	134.47			
28w				0.87	118.39	145.65	0.27	1688.19	1442.62
29w				0.83	124.53	160.91			
30w				0.87	118.39	145.65	0.23	1965.21	1946.02

fracture. The arcuate, *en echelon* segments of the KMF have bisected most of these domes along the northern flanks giving the impression of half dome. The bedding planes of the sediment sequence along the northern flanks of these half domes either dip steeply to north or have become vertical. These results suggest that the Banni region might have continued to be part of the Kachchh Mainland highland till late Palaeogene. These highlands possibly restricted the Deccan basalt flows to the south (Sen et al., 2009).

The shallow seismic studies using microtremor distinguish a cluster of four faults (F_1 , F_2 , F_3 and F_4) along Loriya–Bhirandiara profile from stations 1a to 19w defining 9.5 km wide KMFZ within the Banni Footwall Syncline that runs parallel to the KMF (Figs. 1 and 6). The cluster analysis of aftershocks associated with the Bhuj earthquake, validates the presence of shallow antecedent faults within the Banni Footwall Syncline belonging to the family of large Kachchh Mainland Fault system (Antolik and Dreger, 2003; Mandal and Hurton, 2007b). Out of the four faults, three faults viz., F_1 , F_3 , and F_4 tend to dip to the north (Banni Footwall Syncline) whereas F_2 dips to the south (Kachchh Mainland Hill Range). F_1 and F_4 are the two major faults that bound the KMFZ depression. Closeness of F_1 to the KMF convinces authors to contemplate F_1 as a segment of the KMF that defines southern margin of the KMFZ and displaces Mesozoic sequence. F_4 bounds northern periphery of the KMFZ restricting the M-B interface northerly and raises the basement to a shallower depth. Also, F_4 juxtaposes the younger Jumara Formation extended from the Kachchh Mainland against the older Kaladonger Formation extending from the Patcham Island (see Fig. 3 in Biswas, 1999). The present study correlates F_4 as the

subsurface signature of the Banni Fault mapped by Biswas and Deshpande (1970). The thickness of the Quaternary and the Tertiary-Mesozoic sequence abruptly escalates in the KMFZ. Analogous augment in thickness is recorded in the Deep Nirona Core B (DGH record) further west of the profile along the KMF. The KMFZ shows subsidence whereas uplift to the north (Patcham Island) holds M-B interface high. F_2 and F_3 disrupt the Q-T interface restricting it within the KMFZ. The uplifted, tilted block bounded by F_2 and F_3 suggests structural inversion. The focal mechanism studies from the aftershocks associated with the Bhuj earthquake, further corroborates compressive regime leading to inversion tectonics (Chung and Gao, 1995; Antolik and Dreger, 2003).

The overall geometry of the imbricate faults (F_1 , F_2 , F_3 and F_4) that have deformed the Q-T interface signifies a positive flower structure (Harding, 1985; Woodcock and Fischer, 1986; McClay and Bonora, 2001; Woodcock and Rickards, 2003). Such zones are comparable to step-overs develop along the restraining bends. These step over structures display push-ups because of localized shortening that occurs between two converging bends (Harding, 1974; Christie-Blick and Biddle, 1985; McClay and Bonora, 2001). Analogous consensus attained from the studies in the Wagad Block reveal presence of anastomosing fault pattern, subsurface wrench faulting associated with contractional (restraining bend: Chitrod dome) and extensional bends (releasing bends: Gamdau syncline) within the SWF zone (Kothiyari et al., 2016). Fig. 3 in Biswas (2005) describes positive flower structure along Jhurio Dome–Banni Profile where the Kachchh Mainland Uplift Block and the Wagad Uplift Block shows right lateral strike-slip movement.

The subsurface profile along the Banni Footwall Syncline suggests

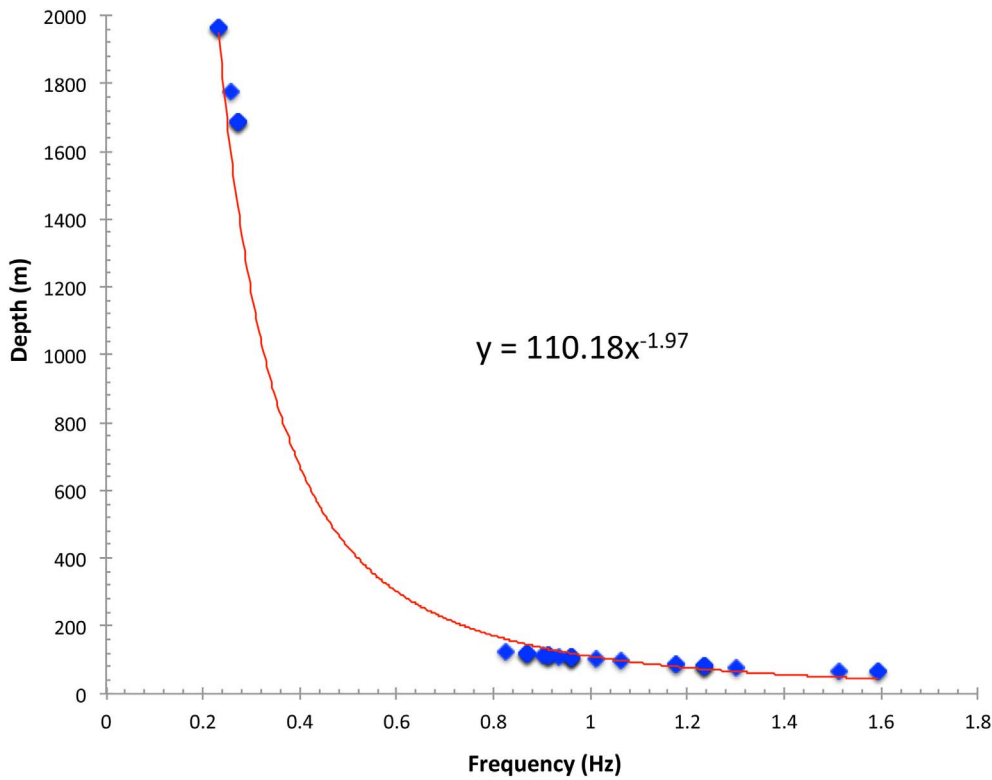


Fig. 4. Scatter plot of fundamental resonating frequency versus calculated depths (calculated based on V_s). The power function trendline for the plots provides a general equation for Banni Plains.

presence of at least two episodes of deformations. The initial event led to the subsidence within the KMFZ bringing Mesozoic sequence juxtaposed to the Basement rocks (F_4). However, the later event led to development of a positive flower structure in the KMFZ (F_1 to F_4).

5. Conclusions

- (1) Shallow seismic studies using microtremors distinguish the Quaternary-Tertiary interface and the Mesozoic-Basement

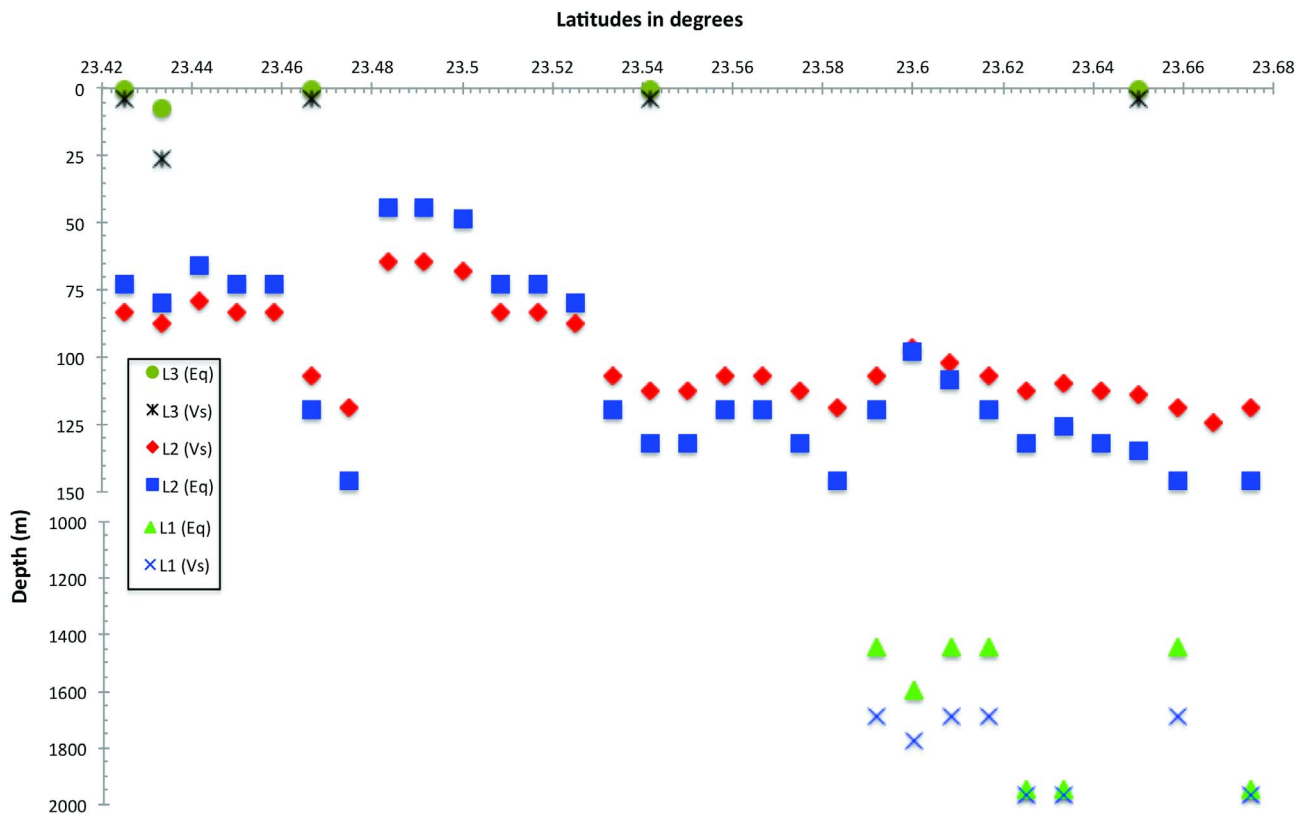


Fig. 5. Comparison of depths calculated for thirteen-one stations using both (1) V_s (1830 km/sec at the M-B interface and 411 km/sec at the Q-T interface) and (2) equation derived for Banni Plain $h = 110.18f_r^{-1.97}$. L1 (Vs) and L1 (Eq) represent M-B interface; L2 (Vs); L2 (Eq) represents Q-T interface; and L3 (Vs) and L3 (Eq) represent other shallow interface.

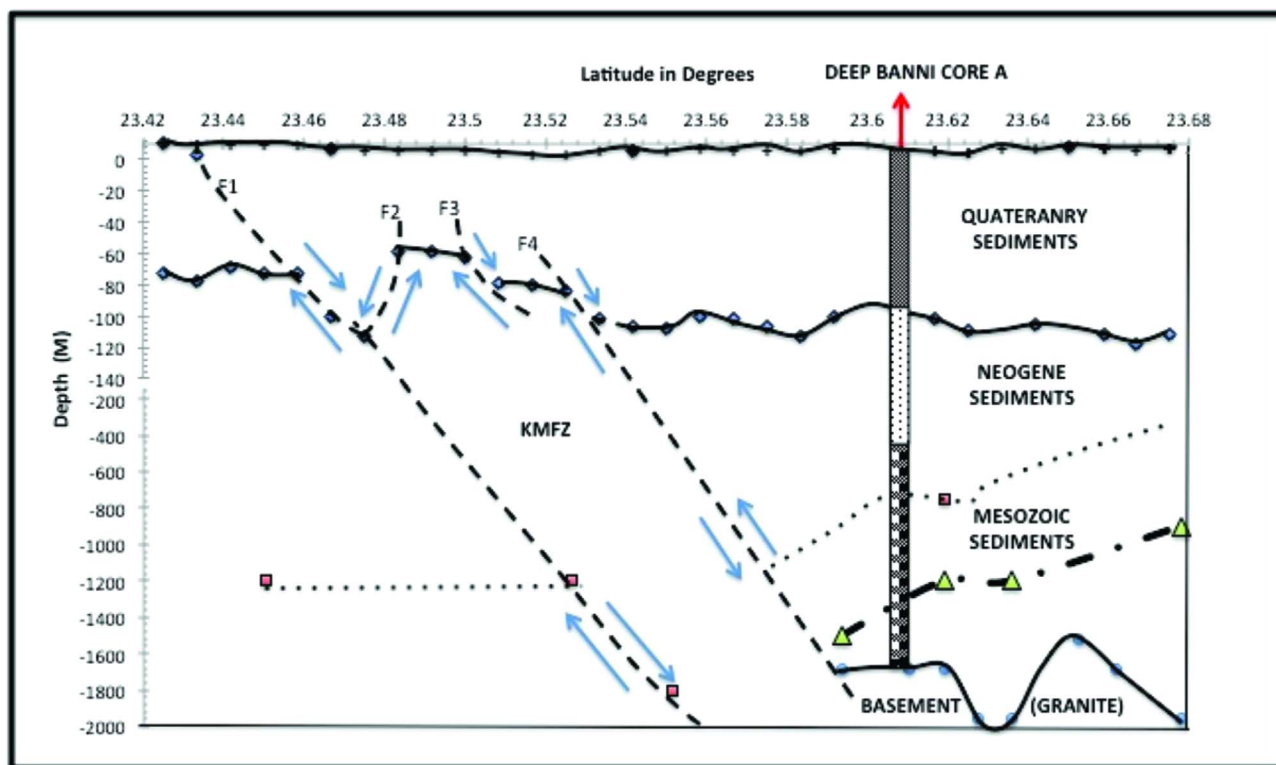


Fig. 6. Three layer model for Loriya –Bhirandiara Profile, Banni Plains. The profile highlights M-B and Q-T interfaces. M-B interface is restricted to the north of Kachh Mainland Fault Zone. The dotted line shows the top of Jumara Formation whereas dot-dash-dot line shows the top of Kaladongar Formation (record taken from Fig. 3 of Biswas, 1999). Column represents the station 23w correlated with Deep Banni Core A. F₁, F₂, F₃ and F₄ represents an array of imbricate faults within Banni Footwall Syncline. The Q-T interfaces shows positive flower structure within Kachh Mainland Fault Zone.

interfaces along Loriya –Bhirandiara profile in the Banni Plains.

- (2) The estimated thickness of the Quaternary sediment varies from 35 m to 115 m whereas thickness of the combined Tertiary and the Mesozoic sequence together varies between 1624 m and 1841 m along profile.
- (3) Microtremor studies along with the DGH Deep Core Record (Deep Banni Core A and Deep Nirona Core B) confirm that the Tertiary sedimentary overlie the Mesozoic sediments and the Deccan basalt flows are absent in the Banni Plains.
- (4) The studies identify the KMFZ as categorized by four imbricate faults (F₁, F₂, F₃, and F₄) that disrupt both Q-T and M-B interfaces. The general geometry of the fault cluster signifies a positive flower structure comparable to step-overs, restraining bends that display push-ups because of localized shortening which occurs between two converging bends.
- (5) The study highlights presence of at least two episodes of deformations in the Banni Footwall Syncline. The initial event led to the subsidence within the KMFZ bringing Mesozoic sequence juxtaposed to the Basement rocks (F₄). However, the later event led to development of a positive flower structure in the KMFZ (F₁ to F₄).

Acknowledgements

DAS, SJP, MNB, and TAS thank Prof. L.S. Chamyal, Head, Department of Geology, The Maharaja Sayajirao University of Baroda, his kind support and encouragement during tenure of research work. DAS thanks DGH for supporting research by supplementing stratigraphic record for Deep Exploratory Cores in study area. I.A.P. thanks Head, CSIR 4PI for his support and encouragement. GR was supported by JC Bose National Fellowship and UGC Centre for Advanced Studies. GR is a Honorary Professor at the Jawaharlal Nehru Centre for Advanced Scientific Research, Bangalore. We thank Dr. D.K. Dasgupta, (ONGC Chair Professor, Department of Geology, The Maharaja

Sayajirao University of Baroda) for reviewing the manuscript. We thank the anonymous reviewer and editor for suggestions to upgrading manuscript.

References

- Aki, K., Richards, P.G., 2002. Quantitative Seismology, second ed. University Science Book. pp. 687.
- Antolik, M., Dreger, D.S., 2003. Rupture process of the 26 January 2001 Mw 7.6 Bhuj, India, earthquake from teleseismic broadband data. *Bull. Seismol. Soc. Am.* 93, 1235–1248.
- Bardan, S., Datta, K., 1987. Biostratigraphy of Jurassic Chari Formation, a study in Keera dome, Kutch, Gujarat. *J. Geol. Soc. India* 30, 121–131.
- Biswas, S.K., 1982. Rift basin in western Margin of India and their hydrocarbon prospects with special reference to Kutch Basin. *Am. Assoc. Petrol. Geol. Bull.* 66, 1497–1513.
- Biswas, S.K., 1987. Regional tectonic framework, structure and evolution of the western marginal basins of India. *Tectonophysics* 135, 307–327.
- Biswas, S.K., 1992. Tertiary stratigraphy of Kutch. *J. Pal. Soc. India* 37, 1–29.
- Biswas, S.K., 1999. A review on the evolution of rift basins in India during Gondwana with special reference to western Indian Basins and their Hydrocarbon prospects. *PINSA* 65(A), 261–283.
- Biswas, S.K., 2002. Structure and Tectonics of the Kutch Basin, Western India with Special Reference to Earthquakes. Eighth IGC Foundation Lecture, Indian Geological Congress, Roorkee, India.
- Biswas, S.K., 2005. A review of structure and tectonics of Kutch basin, western India, with special reference to earthquakes. *Curr. Sci.* 88, 1592–1600.
- Biswas, S.K., 2016. Mesozoic and tertiary stratigraphy of Kutch* (Kachh) – A review. *Spec. Publ. J. Geol. Soc. India* 6, 1–24.
- Biswas, S.K., Deshpande, S.V., 1968. The basement of Mesozoic sediments of Kutch, western India. *Bull. Geol. Min. Metall. Soc. India* 40, 1–7.
- Biswas, S.K., Deshpande, S.V., 1970. Geological and tectonic maps of Kachh. *Bull. Oil Nat. Gas Commis.* 7, 115–116.
- Biswas, S.K., Khatri, K.N., 2002. A geological study of earthquakes in Kutch, Gujarat, India. *J. Geol. Soc. India* 60, 131–142.
- Bard, P.Y., 2008. The H/V technique: capabilities and limitations based on the results of the SESAME project. *Bull. Earthq. Eng.* 6, 1–2.
- Bonnefoy-Claudet, S., Cornou, C., Bard, P.Y., Cotton, F., Moczo, P., Kristek, J., Fäh, D., 2006. H/V ratio: a tool for site effects evaluation. Results from 1-D noise simulations. *Geophys. J. Int.* 167, 827–837.
- Celebi, M., Dietel, C., Prince, J., Onate, M., Chavez, G., 1987. Site amplification in Mexico City (determined from 19 September 1985 strong-motion records and from recording

- of weak motions). *Ground Mot. Eng. Seismol.* 141–152.
- Chandrasekhara, E., Mathew, G., Harinarayana, T., 2012. A new hypothesis for the deep subsurface structures near the Bhuj 2001 earthquake (M_w 7.6) hypocentre zone and its tectonic implications. *Geophys. J. Int.* 190, 761–768.
- Chopra, S., Choudhury, P., 2011. A study of response spectra for different geological conditions in Gujarat, India. *Soil Dynam. Earthq. Eng.* 31, 1551–1564.
- Chopra, S., Kumar, D., Rastogi, B.K., Choudhury, P., Yadav, R.B.S., 2013. Estimation of site amplification functions in Gujarat region, India. *Nat. Hazards* 65, 1135–1155.
- Chowksey, V., Maurya, D.M., Joshi, P., Khonde, N., Das, A., Chamyal, L.S., 2011. Lithostratigraphic development and neotectonic significance of the Quaternary sediments along the Kachchh Mainland Fault (KMF) zone, western India. *J. Earth Syst. Sci.* 120, 979–999.
- Christie-Blick, N., Biddle, K.T., 1985. Deformation and basin formation along strike-slip faults. In: Biddle, K.T., Christie-Blick, N. (Eds.), *Strike-slip Deformation, Basin Formation, and Sedimentation*. Society of Economic Paleontologists and Mineralogists Special Publication No. 37, pp. 1–34.
- Chung, W.Y., Gao, H., 1995. Source parameters of the Anjar earthquake of July 21 1956, India and its seismotectonic implications for the Kutch rift basin. *Tectonophysics* 242, 281–292.
- Delgado, J., Lopez Casado, C., Estevez, A., Giner, J., Cuenca, A., Molina, S., 2000. Mapping soft soils in the Segura River valley (SE Spain): a case study of microtremors as an exploration tool. *J. Appl. Geophys.* 45, 19–32.
- Dinesh, B.V., Nair, G.J., Prasad, A.G.V., Nakkeeran, P.V., Radhakrishna, M.C., 2010. Estimation of sedimentary layer shear wave velocity using micro-tremor H/V ratio measurements for Bangalore city. *Soil Dynam. Earthq. Eng.* 30, 1377–1382.
- Field, E.H., Hough, S.E., Jacob, K.H., 1990. Using microtremors to assess potential earthquake site response: a case study in Flushing Meadows, New York City. *Bull. Seismol. Soc. Am.* 80, 1456–1480.
- Field, E., Jacob, K., 1993. The theoretical response of sedimentary layers to ambient seismic noise. *Geophys. Res. Lett.* 20, 2925–2928.
- García-Jerez, A., Luzón, F., Navarro, M., Perez-Ruiz, J.A., 2006. Characterization of the sedimentary cover of the Zafarraya basin, southern Spain, by means of ambient noise. *Bull. Seismol. Soc. Am.* 96, 957–967.
- Harding, T.P., 1985. Seismic characteristics and identification of negative flower structures, positive flower structures and positive structural inversion. *Bull. Am. Assoc. Petrol. Geol.* 69, 582–600.
- Harding, T.P., 1974. Petroleum traps associated with wrench faults. *Bull. Am. Assoc. Petrol. Geol.* 58, 1290–1304.
- Hough, S.E., Field, E.H., Jacob, K.H., 1991. Using Microtremors to Assess Site-specific Earthquake Hazard. *Earthquake Engineering Research Institute*, pp. 385.
- Ibs-von Seht, M., Wohlenberg, J., 1999. Microtremor measurements used to map thickness of soft sediments. *Bull. Seismol. Soc. Am.* 89, 250–259.
- Joshi, A.U., Sant, D.A., Parvez, I.A., Rangarajan, G., Limaye, M.A., Mukherjee, S., Charola, M.J., Bhatt, M.N., Mistry, S.P., 2017. Sub-surface profiling of granite pluton using microtremor method: southern Aravalli, Gujarat, India. *Int. J. Earth Sci.* <http://dx.doi.org/10.1007/s00531-017-1482-9>.
- Kanai, K., 1957. The requisite conditions for the predominant vibration of ground. *Bull. Earthq. Res. Inst.* 35, 457–471.
- Kar, A., 1993. Digital terrain analysis, granulometry and remote sensing of the Banni tract of Kachchh for development related morphological classification. In: Sharma, P.R., Mishra, S.P. (Eds.), *Applied Geomorphology in the Tropics*. Rishi Publications, Varanasi, pp. 87–104.
- Kar, A., 2011. Geomorphology of the arid lands of Kachchh and its importance in land resources planning. In: Bandyopadhyay, S. et al. (Eds.), *Landforms Processes and Environment*, pp. 388–414. ISBN 81-87500-58-1.
- Karanth, R.V., Gadhavi, M.S., 2007. Structural intricacies: emergent thrusts and blind thrusts of Central Kachchh, western India. *Curr. Sci.* 93 (9), 1271–1280.
- Kazmi, A., Khan, R.A., 1973. The Report on the Geology, Mineralogy and Mineral Resources of Nagar-Parkar, Pakistan. Geological Survey Pakistan, Information Releasepp. 64.
- Konno, K., Ohmachi, T., 1998. Ground-motion characteristics estimated from spectral ratio between horizontal and vertical components of microtremor. *Bull. Seismol. Soc. Am.* 88, 228–241.
- Kothyari, G.C., Dumka, R.K., Singh, A.P., Chauhan, G., Thakkar, M.G., Biswas, S.K., 2016. Tectonic evolution and stress pattern of South Wagad Fault at the Kachchh Rift Basin in western India. *Geol. Mag.* 1–13.
- Khan, T., Murata, M., Hafiz Ur Rehman, H.U., Zafar, M., Ozawa, H., 2012. Nagarparker granites showing Rodinia remnants in the southeastern part of Pakistan. *J. Asian Earth Sci.* 59, 39–51.
- Kumar, S., Chopra, S., Choudhury, P., Singh, A.P., Yadav, R.B.S., Rastogi, B.K., 2012. Ambient noise levels in Gujarat State (India) seismic network. *Geomatics. Nat. Hazards Risk* 3 (4), 342–354.
- Lermo, J., Rodriguez, M., Singh, S.K., 1988. The Mexico earthquake of September 19, 1985 natural period of sites in the valley of Mexico from microtremor measurements and strong motion data. *Earthq. Spectra* 4, 805–814.
- Lunedei, E., Albarello, D., 2010. Theoretical HVSR curves from full wave field modeling of ambient vibrations in a weakly dissipative layered Earth. *Geophys. J. Int.* 18, 1093–1108.
- Maurya, D.M., Khonde, N., Das, A., Chowksey, V., Chamyal, L.S., 2013. Subsurface sediment characteristics of the Great Rann of Kachchh, western India based on preliminary evaluation of textural analysis of two continuous sediment cores. *Curr. Sci.* 104 (8), 1071–1077.
- Malik, J.N., Morino, M., Mishra, P., Bhuiyan, C., Kaneko, F., 2008. First active fault exposure identified along Kachchh Mainland Fault: evidence from trench excavation near Lodai village, Gujarat, Western India. *J. Geol. Soc. India* 71, 201–208.
- Mallik, J., George Mathew, G., Greiling, R.O., 2009. Magnetic fabric variations along the fault related anticlines of Eastern Kachchh, Western India. *Tectonophysics* 473 (3–4), 428–445.
- Mathew, G., Singhvi, A.K., Rama, V., Karanth, R.V., 2006. Luminescence chronometry and geomorphic evidence of active fold growth along the Kachchh Mainland Fault (KMF), Kachchh, India. *Tectonophysics* 422, 71–87.
- Mandal, P., Chadha, R.K., Satyamurty, C., Raju, I.P., Kumar, N., 2005. Estimation of site response in Kachchh, Gujarat, India, region using H/V spectral ratios of aftershocks of the 2001 M_w 7.7 Bhuj earthquake. *Pure Appl. Geophys.* 162, 2479–2504.
- Mandal, P., 2007. Sediment thicknesses and Q_s vs. Q_p relations in the Kachchh Rift Basin, Gujarat, India using Sp converted phases. *Pure Appl. Geophys.* 164, 135–160.
- Mandal, P., Hurton, S., 2007. Relocation of aftershocks, focal mechanisms and stress inversion: implications toward the seismo-tectonics of the causative fault zone of M_w 7.6 2001 Bhuj earthquake (India). *Tectonophysics* 429, 61–78.
- McClay, K., Bonora, M., 2001. Analog models of restraining stepovers in strike-slip fault systems. *Bull. Am. Assoc. Petrol. Geol.* 85, 233–260.
- Naganjaneyulu, K., Ledo, J.J., Queralt, P., 2010. Deep crustal electromagnetic structure of Bhuj earthquake region (India) and its implications. *Geol. Acta* 8 (1), 83–97.
- Nakamura, Y., 1989. A method for dynamic characteristics estimation of subsurface using microtremor on the ground surface. *Quart. Rep. Railway Tech. Res. Inst.* 30, 25–33.
- Nakamura, Y., 2008. On the H/V spectrum. In: *The 14th World Conference on Earthquake Engineering, October 12–17, 2008, Beijing, China*, pp. 1–10.
- Nogoshi, M., Igarashi, T., 1971. On the amplitude characteristics of microtremor (part 2). *J. Seismol. Soc. Jpn.* 24, 26–40.
- Ohta, Y., Kagami, H., Goto, N., Kudo, K.A., 1978. Observation of 1- to 5-second microtremors and their application to earthquake engineering. Part I: comparison with long-period accelerations at the Tokachi-oki earthquake of 1968. *Bull. Seismol. Soc. Am.* 68, 767–779.
- Parolai, S., Bormann, P., Milkereit, C., 2002. New relationships between V_s , thickness of sediments, and resonance frequency calculated by the H/V ratio of seismic noise for the Cologne area (Germany). *Bull. Seismol. Soc. Am.* 92, 2521–2527.
- Parolai, S., Galiana-Merino, J.J., 2006. Effect of transient seismic noise on estimates of h/v spectral ratios. *Bull. Seismol. Soc. Am.* 96, 228–236.
- Paudyal, Y.R., Ryuichi, Y.R., Bhandary, N.P., Dahal, R.K., 2013. Basement topography of the Kathmandu Basin using microtremor observation. *J. Asian Earth Sci.* 62, 627–637.
- Pilz, M., Parolai, S., Leyton, F., Campos, J., Zschau, J., 2009. A comparison of site response techniques using earthquake data and ambient seismic noise analysis in the large urban areas of Santiago de Chile. *Geophys. J. Int.* 178 (2), 713–728.
- Rošer, J., Gosar, A., 2010. Determination of Vs30 for seismic ground classification in The Ljubljana Area, Slovenia. *Acta Geotech. Slov.* 1, 63–76.
- Sastry, R.S., Nagarajan, N., Sarma, V.S., 2008. Electrical imaging of deep crustal features of Kutch, India. *Geophys. J. Int.* 172, 934–944.
- Sánchez-Sesma, F.J., Rodríguez, M., Iturrarán-Viveros, U., Luzón, F., Campillo, M., Margerin, L., García-Jerez, A., Suarez, M., Santoyo, M.A., Rodríguez-Castellanos, A., 2011. A theory for microtremor H/V spectral ratio: application for a layered medium. *Geophys. J. Int.* 186, 221–225.
- Sen, G., Bizimis, M., Das, R., Paul, D.K., Ray, A., Biswas, S., 2009. Deccan plume, lithosphere rifting, and volcanism in Kutch, India. *Earth Planet. Sci. Lett.* 277, 101–111.
- Sen, G., Hames, W.E., Paul, D.K., Biswas, S.K., Ray, A., Sen, I.S., 2016. Pre-Deccan and Deccan magmatism in Kutch, India: implications of new $^{40}\text{Ar}/^{39}\text{Ar}$ ages of intrusions. *Spec. Publ. J. Geol. Soc. India* 6, 211–222.
- SESAME European Project EVG1-CT-2000-00026, 2004. GEOPSY Software – Download Site. < <http://www.geopsy.org> > .
- Sukumaran, P., Parvez, I.A., Sant, D.A., Rangarajan, G., Krishnan, K., 2011. Profiling of late Tertiary–early Quaternary surface in the lower reaches of Narmada valley using microtremors. *J. Asian Earth Sci.* 41, 325–334.
- Singh, A.P., Annam, N., Kumar, S., 2014. Assessment of predominant frequencies using ambient vibration in the Kachchh region of western India: implications for earthquake hazards. *Nat. Hazards* 73, 1291–1309.
- Vedanti, N., Pandey, O.P., Srivastava, R.P., Mandal, P., Kumar, S., Dimri, V.P., 2011. Predicting heat flow in the 2001 Bhuj earthquake ($M_w = 7.7$) region of Kachchh (Western India), using an inverse recurrence method. *Nonlinear Process. Geophys.* 18, 611–625.
- Woodcock, N.H., Fischer, M., 1986. Strike-slip duplexes. *J. Struct. Geol.* 8, 725–735.
- Woodcock, N.H., Rickards, B., 2003. Transpressive duplex and flower structure: Dent Fault System, NW England. *J. Struct. Geol.* 25, 1981–1992.
- Yamanaka, H., Takemura, M., Ishida, H., Niwa, M., 1994. Characteristics of long-period microtremors and their applicability in exploration of deep sedimentary layers. *Bull. Seismol. Soc. Am.* 84, 1831–1841.
- Zhao, B., Xie, X., Chai, C., Ma, H., Xu, X., Peng, D., Yin, W., Tao, J., 2007. Imaging the graben structure in the deep basin with a microtremor profile crossing the Yinchuan City. *J. Geophys. Eng.* 4, 293–300.